LARGE-SCALE EXPERIMENT ON DYNAMIC RESPONSE OF SAND BED AROUND A CYLINDER DUE TO TSUNAMI

Fuminori KATO[1], Shinji SATO[2] and Harry YEH[3]

Abstract

The scour process around a vertical cylinder due to tsunami runup was investigated experimentally using a large-scale laboratory facility. Temporal variations of scouring around the cylinder were optically observed with the multiple CCD cameras that were installed inside of the cylinder. All the other necessary data, e.g. water depth, flow velocity and pore pressure, were obtained by the conventional electronic sensors. In addition, we measured the topography changes before and after the tsunami runup. The temporal variations of the scour process were clarified. It was found that the pore pressure field around the cylinder is one of the key factors to understand scouring mechanism associated with tsunami runup.

Introduction

It is well known that a tsunami attack causes substantial erosion and scour on the shore. For example, the 1960 Chilean tsunami scoured out the port entrance by more than 10 m at Kesen-numa Port in Japan. Recent tsunami surveys, from the 1992 Nicaragua tsunami to the 1998 Papua New Guinea tsunami, also discovered substantial tsunami scouring effects around structures and trees. In fact, scouring is sometimes the primary cause of structure damage and destruction.

It is likely that the tsunami-scour process around on-shore structures is different from the present understanding of bridge-pier-type scour processes in river and coastal

[1]Research Engineer, Coast Division, Public Works Research Institute, Asahi 1, Tsukuba 305-0804, Japan

[2]Professor, Department of Civil Engineering,University of Tokyo, Hongou 7-3-1, Bunkyo-ku, Tokyo 113-8656, Japan

[3]Professor, Department of Civil and Environmental Engineering, University of Washington, Box 352700, Seattle, Washington 98195-2700, U.S.A.

environments. Flows associated with tsunami runup are far from being steady or uniform, and the scouring takes place over a short duration, often less than fifteen minutes. It is also important to recognize that the onshore soil (sediments) conditions during tsunami runup are initially unsaturated and suddenly become wet on the surface while the majority of pore spaces are still filled with air.

This complex problem must be approached experimentally to understand the physics and mechanisms of scour phenomena associated with tsunami runup. Final scour depths were often measured by field observation after tsunami attack, however, it is difficult to measure the scour depths during tsunami runup and drawdown on site. Scouring during tsunami runup and drawdown can be deeper than that after tsunami attack because sand deposition could occur during tsunami drawdown. For the design criteria for coastal structures, the maximum scour depth during tsunami runup process is more important rather than final scour depth.

The previous investigations of tsunami scouring processes are limited. Uda et al. (1987) found that scouring near a revetment due to tsunamis is governed by the topography behind the revetment. As for scouring in front of a revetment, Nishimura and Horikawa (1979) and Noguchi et al. (1997) found some correlation between the scour depth and the water depth in front of the revetment in the tsunami drawdown process.

For our study, we chose a simple and generic shape of the structure, i.e. a cylinder. A cylindrical shaped object may represent, for example, a tree, an onshore oil storage tank, etc. Because the scale effects could be important for this type of experiments, a sufficiently large experimental facility was used.

Experimental Condition

A series of experiments was performed in a 135 m long, 2 m wide, 5 m deep sediment tank at Public Works Research Institute, Tsukuba, Japan. To generate a wide variety of long waves, the tank is equipped with the piston-type wave-maker driven by a large servo motor. The maximum stroke of the wave paddle is 2.4 m with the maximum speed of 1.11 m/s. It was tested and proven to generate a clean solitary wave of at least 40 cm high in a 3 m water depth. A beach of well-graded sediment (approximately D_{50} = 0.35 mm sand particles) was constructed with a uniform slope of 1/20. As shown in Figure 1, the model cylinder was placed upright on the beach. The cylinder is 50 cm in diameter, made of 1 cm thick Plexiglas, water tight at the bottom end, and connected above to the aluminum cylinder in order to assure its stiffness. Because of the transparent cylinder wall, the scour process can be recorded from the interior with three miniature CCD video cameras, which cover more than 180-degree view of the circumference from the upstream to the downstream sides. Wave gages, an electromagnetic flow meter and pore pressure transducers were placed as shown in Figure 2. In addition, before and after each experiment, topography surveys were conducted in the 4 m by 1 m region around the cylinder.

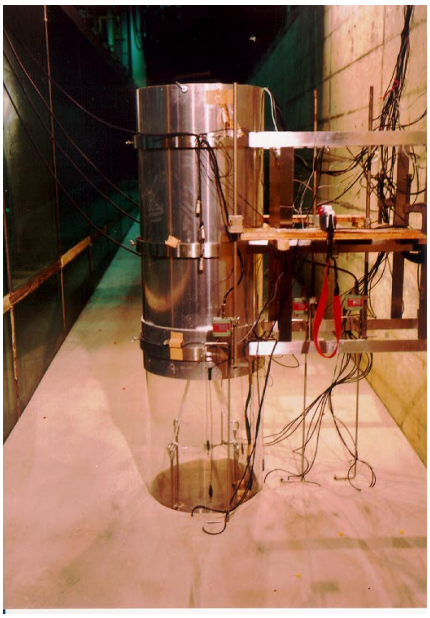

Figure 1. A view of the model cylinder and its support system used for the experiments

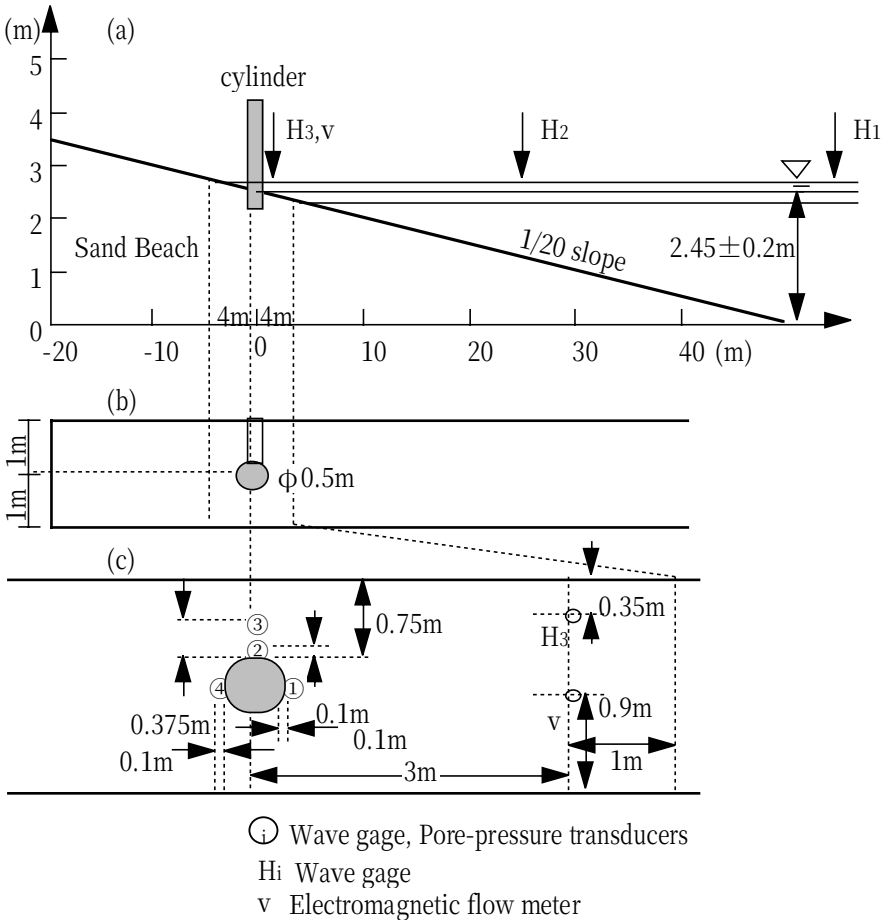

Figure 2. Schematic elevation and plan views of the experimental set-up

Table 1. Experiment condition

Case	WaterDepth(m)	WaveHeight(m)	a/h	RunupHeight(m)	
1	2.25	0.29	0.13	0.695	
2	2.45	0.32	0.13	0.755	
3	2.65	0.34	0.13	0.765	
4	2.25	0.20	0.09	0.580	
5	2.45	0.22	0.09	0.610	
6	2.65	0.24	0.09	0.650	
7	2.25	0.11	0.05	0.420	
8	2.45	0.12	0.05	0.435	
9	2.65	0.13	0.05	0.465	
10	2.65	0.24	0.09	0.670	no cylinder
11	2.45	0.22	0.09	0.660	no cylinder

The experiments were performed for total 11 cases as listed in Table 1. Note that the last two cases in Table 1 are those for the plane beach without placing the cylinder. The nonlinearity of the incident solitary wave was parameterized by the ratio (a/h) of wave height a to the offshore water depth h. Three different incident wave conditions were used in terms of the nonlinear parameter: a/h = 0.13 (cases 1, 2 and 3), 0.09 (cases 4, 5, and 6), and 0.05 (cases 7, 8, and 9). Three different offshore water depths were used: 2.25 m for the case 1, 4 and 7, 2.45 m for the case 2, 5 and 8, 2.65 m for the case 3, 6 and 9. Since the position of the model cylinder is fixed throughout the experiments, the offshore water depths, h = 2.25 m, 2.45 m and 2.65 m, correspond with the cylinder location at 4 m onshore from the still shoreline, on the shoreline and at 4 m offshore, respectively.

In order to evaluate the effect of existence of the cylinder, the maximum runup heights were measured with and without the cylinder placement using the identical incident wave condition. Under the condition of 2.65 m offshore water depth, the maximum runup height of Case 6 (with the cylinder) is 2 cm lower than Case 10 (without the cylinder). With 2.45 m offshore water depth, the runup of Case 5 (with the cylinder) is 5 cm lower than Case 11 (without the cylinder). These results indicate that the presence of the cylinder reduces the tsunami runup height very slightly, which indicates that the blockage of the runup motion by the cylinder is negligible and the tank width is considered wide enough to neglect the side-wall effects.

Topography Change due to Tsunami Runup

Before and after each experiment, topography survey was conducted in the area of 1 m wide from the center of the cylinder toward the tank wall, 2 m onshore and 2 m offshore from the center of the cylinder. The measurement interval of 20 cm was used before the experiment, and, after the experiment, the finer interval of 5 cm was used within 50 cm from the cylinder, and 10 cm interval in the rest of the surveyed area.

Figure 3 shows the beach-profile variations a) in the cross-shore direction from the

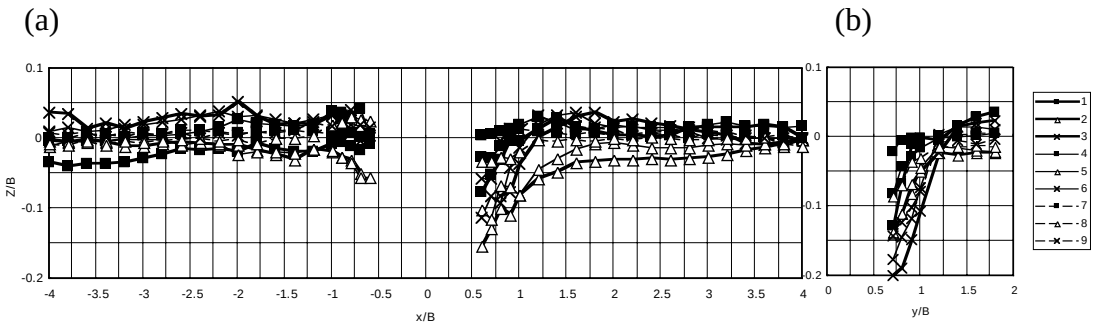

Figure 3. Beach profile variations due to tsunami runup a) in the cross-shore direction and b) in the longshore direction. The positve *x* points the inshore direction. *B* is the cylinder diameter.

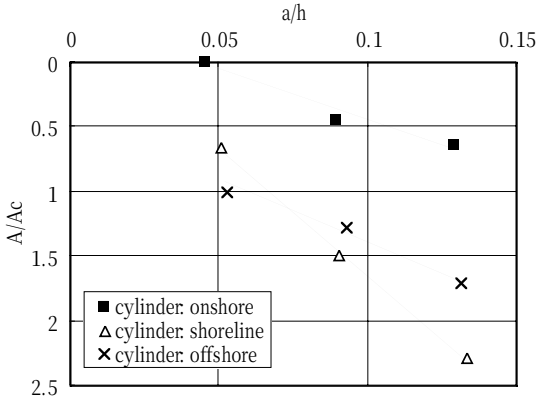

Figure 4. Wave height and scour area

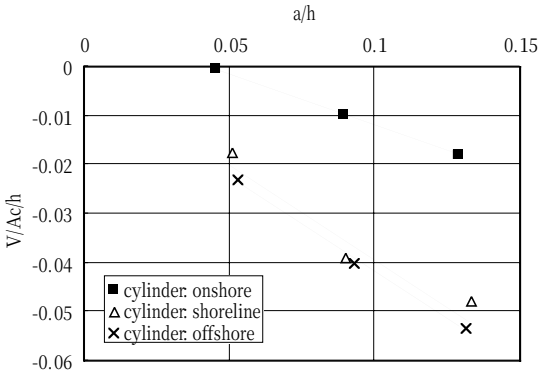

Figure 5. Wave height and scour volume

center of the cylinder, b) in the longshore direction from the cylinder. The positive values indicate deposition and the negative values indicate scour. Figure 3(b) shows the maximum scour in the longshore direction occurs when the cylinder is placed offshore (i.e. the cylinder was submerged initially), while Figure 3(a) shows that the scour on the inshore side is maximum when the cylinder is placed at the shoreline. When the cylinder was placed inshore (cases 1, 4 and 7), the least scour occurred. There was no significant scour at the onshore side of the cylinder except Cases 2 and 5, when the incident waves were large and the initial shoreline was at the cylinder. In addition, the larger the wave height, the deeper the scour depth.

Figure 4 shows the relation between the incident wave height and the area of scour depth more than 2 cm deep. Note that the scour area was normalized by the area of the cylinder, and the wave height was normalized by the initial water depth offshore. In comparison with the cases when the cylinder was placed inshore, the scour area was larger when the cylinder was placed on the shoreline or offshore. The scour area appears to be proportional to the wave height; the scour area is much more sensitive to the incident wave height when the cylinder is at the shoreline.

Figure 5 shows the relation between the incident wave height and the sediment volume change in the area near the cylinder. The area of the measurement is 1 m long in the cross-shore direction and 0.5 m wide in the longshore direction with the one edge bisecting the cylinder in the cross-shore direction. The volume was normalized by the cylinder area times the initial water depth offshore. The net volume change for the case with the cylinder being placed inshore is smaller than that the other cases; the changes are comparable for the cases of the cylinder on the shoreline and at the offshore location. The proportionality shown in Figure 5 appears to be similar for all three cases with different locations of the cylinder.

Scouring around a Cylinder elucidated by Video Analysis

To clarify scouring mechanisms around the cylinder, sand response around the cylinder wall was observed with three miniature CCD video cameras installed inside of the cylinder. This can be accomplished because of its large size cylinder model (50 cm in diameter) that is made of a transparent (Plexiglas) cylinder wall.

Typical video images of the sand response around the cylinder wall are shown in Figure 6. The line drawn in the figure indicates the instantaneous location of sand bed. The images on the top of Figure 6 represent the initial condition prior to the tsunami runup, the middle images are those at the maximum inundation, and those on the bottom are after the tsunami drawdown. During the runup, scouring occurred both at the offshore side and longshore side, while scouring did not occur at the onshore side. During the tsunami drawdown, further scouring din not occur at the offshore side, but the scouring progressed at the longshore side. Severe scouring occurred at the onshore side. The scour depths around the cylinder can be determined from these images.

The scour-depth variations at the point facing offshore are shown in Figure 7. The depths are all normalized by the diameter of the cylinder. During the tsunami runup,

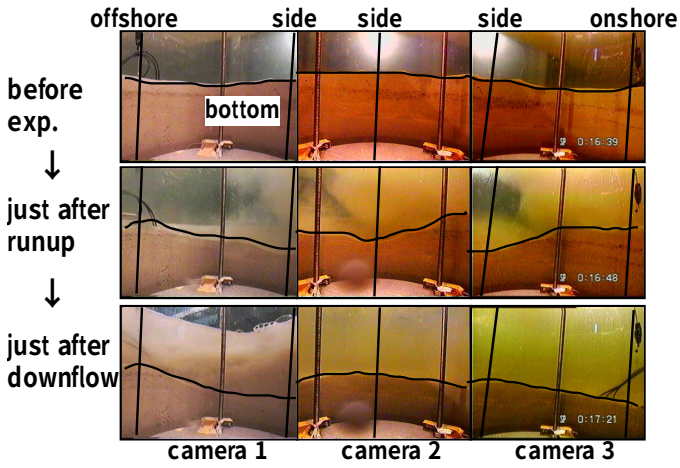

Figure 6. Video images of the scour process obtained with the three miniature CCD cameras placed inside of the cylinder

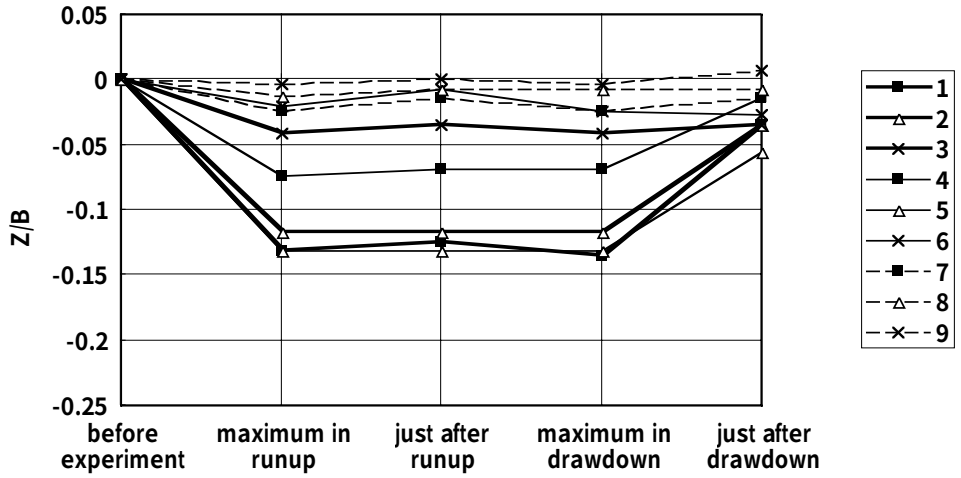

Figure 7. Scour depth at the offshore side

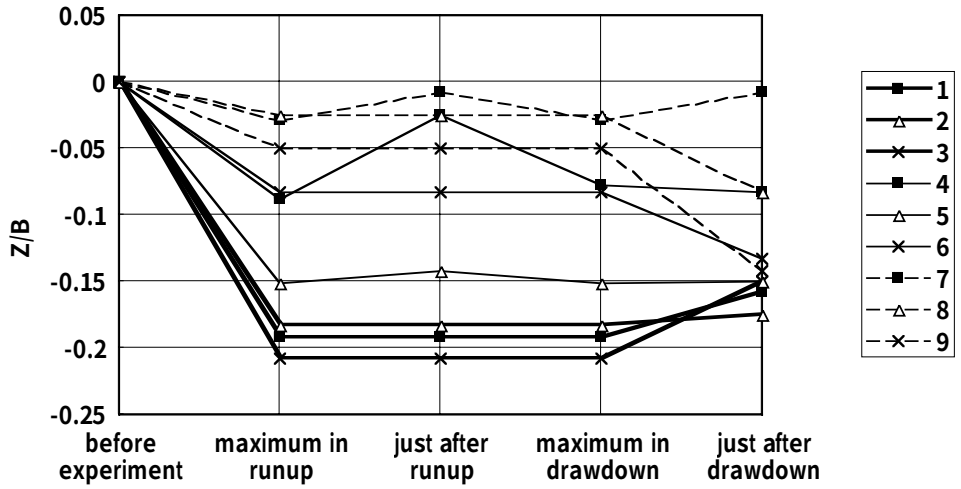

Figure 8. Scour depth at the longshore side

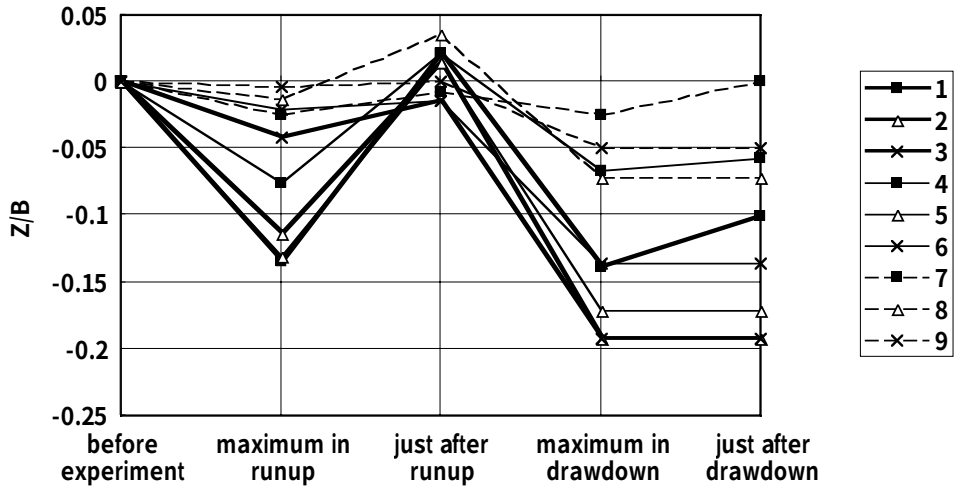

Figure 9. Scour depth at the inshore side

scouring resulted in most cases, i.e. the sand-surface elevation decreased. During the drawdown, sand accumulation occurred in the cases with the large scour depth at the maximum inundation. This behavior is evident in the cases with the cylinder located onshore and at the shoreline; especially in case 4, its scour depth at the maximum inundation is five times as large as that just after tsunami drawdown. At the maximum inundation under the same incident wave condition, i.e. the same ratio of wave height to water depth (a/h), the scour depth was the greatest when the cylinder was placed at the onshore location when $a/h = 0.13$ or 0.05. On the other hand, the maximum scour depth occurred for the cylinder at the shoreline if the incident wave is $a/h = 0.09$, i.e. Case 5. In Case 5, breaking of the incident wave occurred and plunged just in front of the cylinder. Perhaps, this is the reason why the maximum scour occurred when the cylinder was at the shoreline.

Figure 8 shows scour-depth variations (normalized by the cylinder diameter) at the longshore side of the cylinder wall. During the tsunami runup, scouring occurred in all cases. During the tsunami drawdown, sand deposition occurred in Cases 1, 2, and 3 in which the scour depth at the maximum inundation was large; on the other hand, further scouring occurred in the other cases. Comparing Figure 8 with Figure 7, scouring during the runup process is greater at the longshore side of the cylinder than that at the point facing offshore. For the cases with the same incident wave condition, a/h, the scour depth at the maximum inundation is the greatest when the cylinder is placed offshore for $a/h = 0.13$ and 0.05. Note that the maximum scour depths at the offshore side of the cylinder resulted when the cylinder was placed inshore as discussed with Figure 7. On the other hand, with $a/h = 0.09$, the largest scour at the maximum inundation occurred when the cylinder was placed at the shoreline. Again, wave breaking near the shoreline must be the reason for the case of $a/h = 0.09$.

Figure 9 shows scour-depth variations at the point facing in the onshore direction (behind the cylinder). On the contrary to the offshore side and the longshore side presented in Figures 7 and 8, the scour holes were recovered by sand deposition during the tsunami runup. During the tsunami drawdown, severe scouring occurred again. Scour depths after the tsunami drawdown were as large as that of the longshore side at the maximum inundation stage shown in Figure 8. For a given incident wave condition, scour depths after the tsunami drawdown were the greatest in the cases where the cylinder was on the shoreline, and the smallest in the cases where the cylinder was placed at the onshore location.

Relation between Pore Pressure and Scour Process

Soil liquefaction in the seabed is often caused by a time lag between the pore pressure variation in the soil and the water pressure variation on the bed. It is considered that sediments are liquefied when the vertical effective stress vanishes. The vertical effective stress σ'_v can be expressed as

$$\sigma'_v = \sigma'_{v0} + (p_b - p_m) \tag{1}$$

where σ'_{v0} is the initial vertical effective stress, p_b is the water pressure variation on the bed, p_m is the pore pressure variation. In this study, the water pressure variations on the bed are approximated by the assumption of hydrostatic pressure estimated from the instantaneous water level measured with the wave gage. The vertical effective stresses are computed without considering the bed elevation variation during the process, i.e. the constant value of initial effective stress σ'_v was used for the computations. Hence the value of $\sigma'_v = 0$ may not correspond accurately to the state of liquefaction, but it should indicate, at least the condition when sediments become very close to that state and movable.

Temporal variations of the scour depth at the offshore side, longshore side, and inshore side of the cylinder are determined from the video images such as Figure 6. They were plotted at the bottom of Figure 10 for Case 5, that is $a/h = 0.09$ and the cylinder at the shoreline, and in Figure 11 for Case 6, that is $a/h = 0.09$ and the cylinder 4 m offshore from the still shoreline. Also shown in Figures 10 and 11 are temporal variations of horizontal flow velocity at 3 m offshore from the cylinder, and the water depths and the vertical effective stresses (at 10 cm deep) around the cylinder. The wave arrival time at the electromagnetic flow meter is approximately 1 sec. earlier in comparison with the wave gage data at the front face of the cylinder, and the data may not accurately represent the flow conditions around the cylinder. None the less, the velocity data show that the horizontal velocity in the cross-shore direction decelerates linearly after its sudden increase at the arrival of the wave. It is also noticed that the maximum inshore velocity at the arrival has almost the same magnitude as the maximum offshore velocity at the cessation of the drawdown process.

In Figures 10 and 11, the water depth at the offshore side of the cylinder decreases monotonically after its sudden increase caused by the initial tsunami impingement, while the water level at the inshore face maintains to be nearly constant throughout the runup and drawdown processes. At the longshore side of the cylinder, the vertical effective stress in the soil vanishes for most of the runup and drawdown processes, i.e. soil liquefaction must occur there. The vertical effective stress at the inshore side vanishes at the end of the drawdown process when the water depth there starts to be reduced. On the other hand, the vertical effective stress at the offshore side stays positive during the entire process. It is emphasized that the maximum scour depths around the cylinder do not coincide with the final states being resulted after the drawdown. The maximum scour depth occurs during the runup process at the offshore side in Figure 10, whereas at the longshore side and the inshore side the maximum scour occurs near the end of the drawdown process as shown in Figures 10 and 11. The cessation of scour process shown at the longshore side and the inshore side appears to coincide with the termination of zero vertical effective stresses as indicated with the arrow marks in the Figures 10 and 11. After that, the scour depths are reduced quickly to the final depths. Once the vertical effective stresses start to increase and have positive

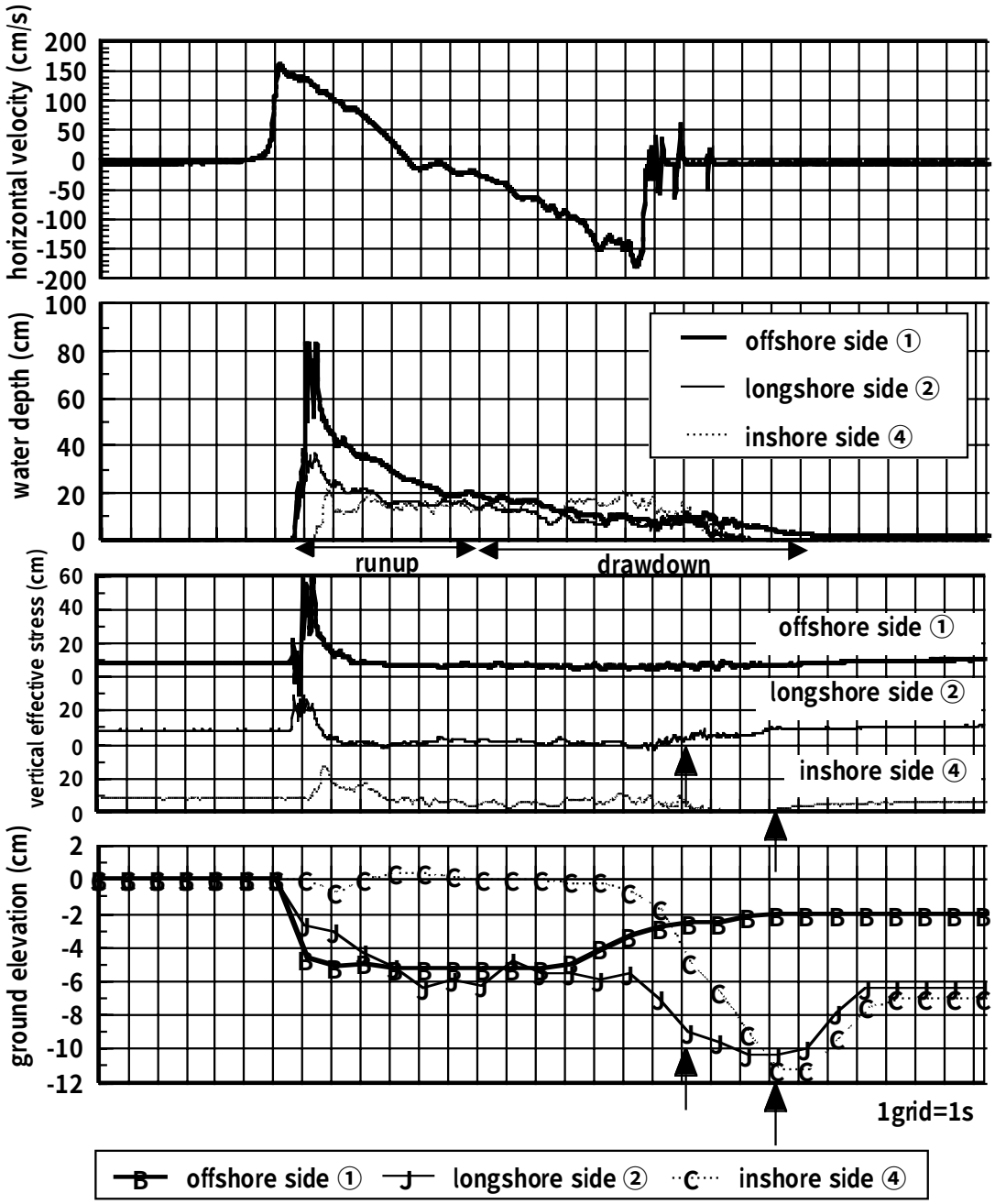

Figure 10. Temporal variations of horizontal velocity, water surface elevations, vertical effective stresses and bed locations. The incident solitary wave has a/h = 0.09 and the cylinder is located at the shoreline.

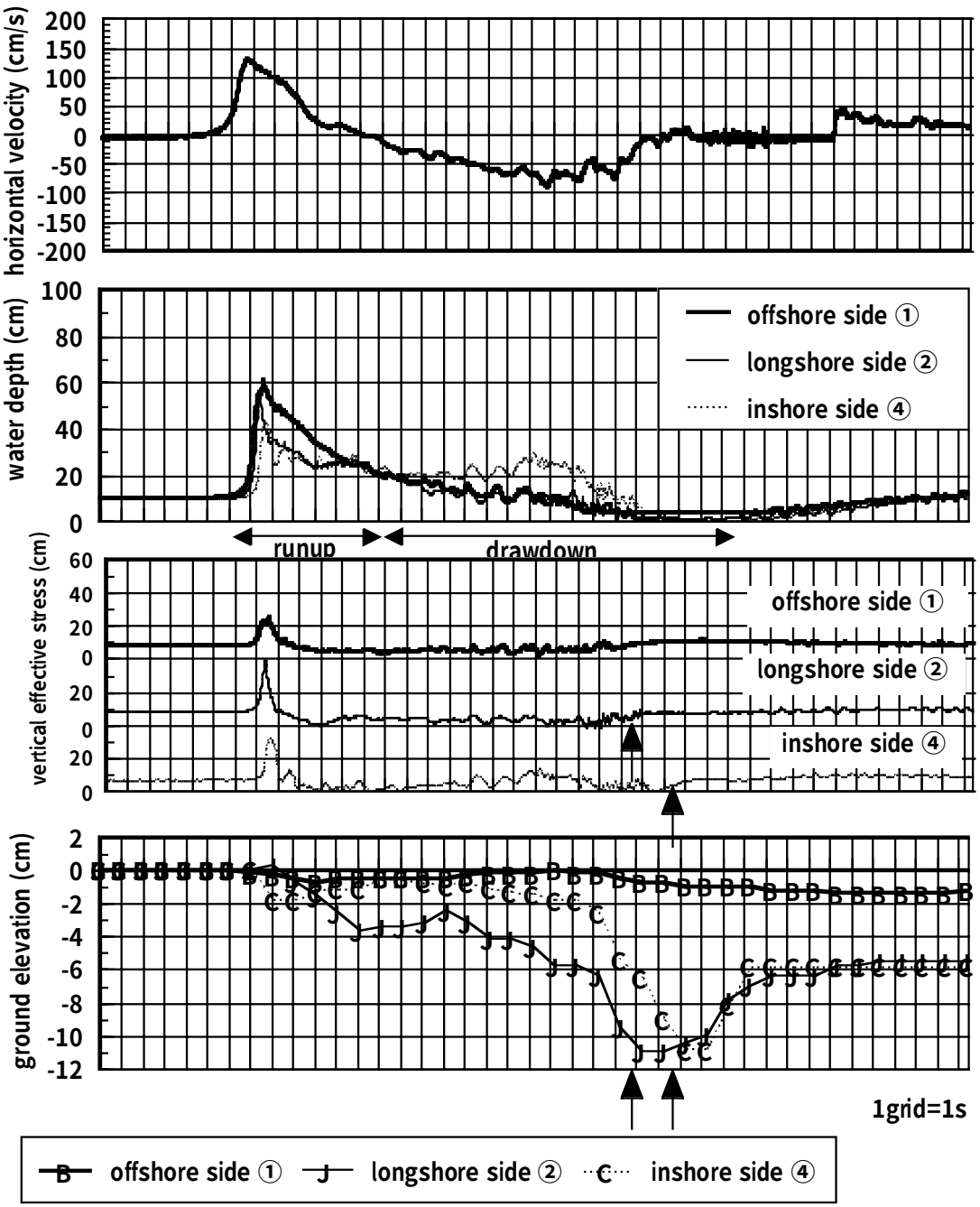

Figure 11. Temporal variations of horizontal velocity, water surface elevations, vertical effective stresses and bed locations. The incident solitary wave has a/h = 0.09 and the cylinder is located 4 m offshore from the still shoreline.

values, the scour holes are immediately recovered with sediments in a short duration of the end stage of the drawdown process.

Conclusions

The principal findings will be summarized as follows:
(1) The scour area and the volume are proportional to the wave height. They are also dependent on the relative location of the cylinder to shoreline.
(2) The scour depth changed dynamically during the tsunami runup and drawdown. In one case, the maximum instantaneous scour depth reached five times the scour depth measured after the tsunami drawdown.
(3) In the seabed near the cylinder, the vertical effective stresses decreased notably during tsunami runup and drawdown processes. The decrease in the vertical effective stress raised fluidity in the bed and played an important role in scouring due to a tsunami attack on the shore.

References

Nishimura H., K. Horikawa (1979) : Scouring at the toe of a seawall due to tsunami drawdown, Proceedings of the 26th coastal engineering conference, pp. 210-214. (in Japanese)
Noguchi K., S. Sato and S. Tanaka (1997) : Large-scale experiments on wave overtopping and scouring at the toe of seawall, Proceedings of the 44th coastal engineering conference, pp. 296-300. (in Japanese)
Uda, T., A. Omata and Y. Yokoyama (1987) : Report of experiments on tsunami runup, Technical Memorandum of PWRI, No. 2486, 122 p. (in Japanese)